Engineering Geology 264 (2020) 105334

Contents lists available at ScienceDirect

Engineering Geology

journal homepage: www.elsevier.com/locate/enggeo

Collapsible intact soil stabilisation using non-aqueous polymeric vehicle

Margherita Zimbardo*, Laura Ercoli, Maria Chiara Mistretta, Roberto Scaffaro, Bartolomeo Megna

Department of Engineering, University of Palermo, Italy

ARTICLE INFO

Keywords:
Collapsible Sands
Stabilisation
Compressibility
Shear strength
PEG
Nanolime

ABSTRACT

This paper presents the results of an experimental study that had the goal of understanding the effects of treatment with polyethylene glycol (PEG)/nanolime mixtures on collapsible soil behaviour. In a previous study, the use of pure PEG offered a good improvement in the stability of collapsible soil, but the stabilisation effect only lasted for a limited time. To investigate the stabilisation potential of PEG/nanolime systems for collapsible sand, different mixtures were prepared at increasing nanolime weight ratios. The suitability of the stabilised soil was examined on the basis of collapsibility, oedometer, shear, and water vapour permeability tests, and through optical microscopy and scanning electron microscopy observations. The stabilisation effects were analysed by comparing the mechanical behaviour of the sand before and after each treatment. The results showed that even though using various mixtures had different effects on the behaviour of collapsible soils, the treatment produced a significant change in the geotechnical behaviours of the sand in relation to the collapse potential, permeability, compressibility, and shear strength.

1. Introduction

Collapsible soils undergo a drastic particle rearrangement and considerable and sudden reduction in total volume of the soil mass under a constant normal stress upon wetting (Barden et al., 1973; Mitchell, 1976; Al-Rawas, 2000), upon an increase in normal stress with a constant water content, or upon a combination of these two stress paths (Haeri et al., 2016). The presence of collapsible soil is one of the common causes of uneven foundation settlement. The addition of water to the soil either reduces the soil suction or softens (or destroys) the bonding, thereby causing shear failures at the inter-aggregate or inter-granular contacts (Dudley, 1970).

Many researchers have studied the influence of soil properties, including the microstructure, fabric, initial moisture content, initial dry density, and stress conditions, on the collapsibility of loess soils (Feda, 1966; Houston et al., 2001; Zhang et al., 2004; Pereira et al., 2005; Romero and Simms, 2008). Haeri and Garakani (2012) showed that changes in the water content and deformation during wetting depended on the value of the matric suction.

The hydromechanical behaviour of collapsible soil is influenced by the extent of the applied mean net stress and level of suction (Garakani et al., 2015), and by the specimen disturbance and initial soil structure (i.e., pore-size distribution) (Haeri et al., 2016).

Collapse problems have contributed to serious damage to infrastructures constructed on collapsible soils (Houston et al., 2001; Ping et al., 2016). Cases of collapse have been extensively documented in many parts of the world, and are typically associated with water saturation (Lutenegger and Hallberg, 1988; Gao, 1996).

A collapse problem (i.e.,a potential wetting-induced volume change) is often identified prior to the construction of a structure, and the estimation of the collapse potential is the most important action to distinguish the behaviour of these soils (Kazemi, 2010).

The direct measurement of collapse magnitude using laboratory tests is essential once a soil has shown a collapsible behaviour. Jennings and Knight (1975) classifies soils with collapse potentials greater than 1 % as metastable. Collapse values exceeding 2 % are regarded as indicative of soils susceptible to collapse (Lutenegger and Hallberg, 1988; Zeng and Meng, 2006). The collapse potential increases with a decrease in the initial water content (Haeri et al., 2012). Moreover, the volume reduction progressively increases with the applied stress at the same inundation stress (Nocilla et al., 2013).

Treatment methods such as soil replacement, compaction control, and chemical stabilisation have shown significant reductions in the settlement of collapsible soils. Indeed, these engineering techniques offer different and adaptable mitigation measures to increase the bearing capacity of collapsible soil (Anayev and Volyanick, 1986) by means of removal and partial replacement (Houston and Houston, 1997), pre-wetting (Hansen et al., 1989; Rollins and Rogers, 1994), pre-

* Corresponding author at: Viale delle Scienze, Ed. 8, 90128 Palermo, PA, Italy.
E-mail address: margherita.zimbardo@unipa.it (M. Zimbardo).

https://doi.org/10.1016/j.enggeo.2019.105334
Received 3 April 2019; Received in revised form 6 October 2019; Accepted 11 October 2019
Available online 24 October 2019
0013-7952/

Nomenclature

CP	Collapse Potential	v	Specific volume
Cc	Compression index	v_0	Initial specific volume
Cr	Re-compression index	γ_0	Initial unit weight
c'	Coesion	γ_m	Unit weight of treated sand
DW	Weight variation	γ_s	Unit weight of the sand
dh	Horizontal displacement	γ_{sm}	Unit weight of the solid particles of the mixtures
e_0	Initial void ratio	$\gamma_{s,p}$	Unit weight of the solid particles of PEG 600
f_{nl}	Percentage of nanolime in the mixture	$\gamma_{s,nl}$	Unit weight of the solid particles of nanolime
f_p	Percentage of PEG in the mixture	ε_v	Vertical strain ($\Delta H/H_0$)
n	Porosity	σ'_v	Effective vertical stress
n_m	Volume of absorbed mixture / initial porosity of the sample	τ	Shear stress
		φ'	Angle of shearing resistance

compression, dynamic compaction (Cintra et al., 1986; Clemence and Finbarr, 1981), and grouting (Pengelly et al., 1997; Ziaie Moayed and Kamalzare, 2015).

When the problem concerns structures that are already built on collapsible soil (such as historical or archaeological structures), the previously mentioned techniques are inapplicable because they essentially involve a drastic rearrangement of the soil.

It is therefore necessary to treat the collapsible soils with active or passive agents that can uniformly penetrate into the soil without decreasing the suction. The active stabilising agents, reacting with materials present in the soil, create a homogeneous stabilised mixture, while passive agents react with and mechanically stabilise the soil. Steward et al. (2000) analysed the effects of waterborne polymer treatment to improve the bonding between soil particles. Some waterborne styrene acrylic polymeric emulsions were used by Al-Khanbashi and El-Gamal (2003) to enhance the mechanical properties and reduce the hydraulic conductivity of collapsible sand.

Many studies have investigated the use of polymeric mixtures and consolidants (Rizzo et al., 2009; Otero et al., 2018; Taglieri et al., 2018; Zhu et al., 2019; Idrees et al., 2019; Lin et al., 2019) to mitigate or protect against the surface degradation agents of mortars or soft rocks in the built cultural heritage conservation field. The use of nanoparticles in geotechnical engineering is still an emerging technology. The use of silica nanomaterial for reconstituted soil stabilisation was investigated by Yonekura and Miwa (1993) in order to increase the compressive strength of sand and by Noll et al. (1992) to reduce the soil permeability. Gallagher and Lin (2005) studied the use of silica nanomaterial to increase the soil's cohesion and decrease its permeability. It was found that the behaviour of the sand was improved by the analysed nanomaterials. Recently, technologies have been developed to consolidate limestone by the application of calcium hydroxide nanoparticles, which penetrate into the material (Giorgi et al., 2010). The carbonation process has some positive effects by enhancing the compressive strength (Drdácký et al., 2009). The use of nanolime for stone stabilisation was one of the earlier applications of nanotechnologies in the cultural heritage field. $Ca(OH)_2$ particles with submicrometric dimensions make it possible to obviate to the traditional lime treatment limitations (Dei and Salvadori, 2006; Daniele et al., 2008).

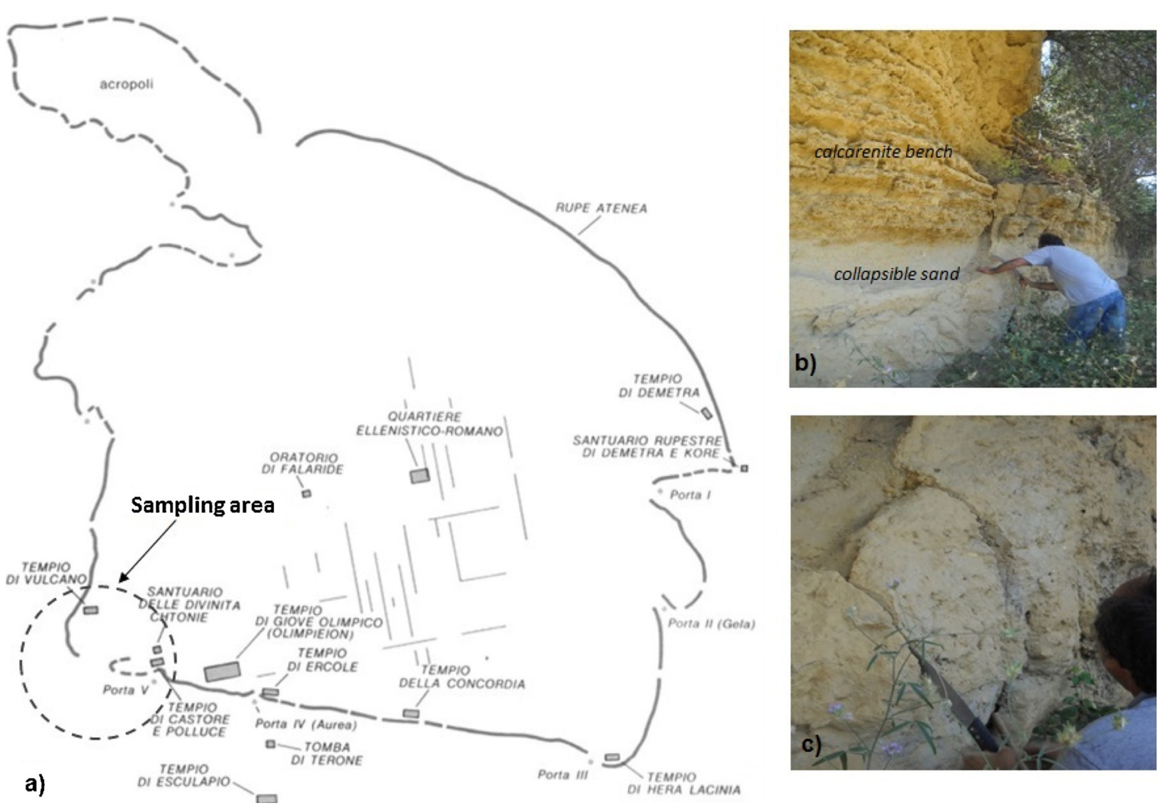

Fig. 1. a)Valle dei Templi in Agrigento: sampling area for collapsible sand, and b), c) sampling sand block by means of saw.

Metastable soils such as loess, desert sand, or liquefiable soils are stabilised to improve their geotechnical properties by means of polymeric mixtures and nanolime stabilisers (Haeri et al., 2015; Kakavand and Dabiri, 2018). Such stabilisation treatment has been performed in the laboratory on reconstituted soils (Hosseini et al., 2012; Saad et al., 2016). These treatments have been able to modify microstructural and mechanical stone characteristics. Haeri et al. (2019) investigated the hydromechanical behaviour of a reconstituted lime-stabilised loessial soil by conducting unsaturated suction-controlled odometer tests and showed that adding a small amount of lime to collapsible loessial soils not only reduced the collapse-induced volume changes to a large extent, but could also increase the yield strength of the soil.

Polymer impregnation has been proven to increase the environmental and mechanical resistance of tuff (a soft pyroclastic rock), producing an improvement in the properties of the material (Aurisicchio et al., 1985; Jiang et al., 2019).

As previously mentioned, the greatest problems with collapsible soils arise either when the existence of the collapse potential is not recognised prior to construction, or when it is necessary to stabilise large volumes such as the collapsible soil foundation of existing structures. This particularly a problem if it is not possible (because of geological factors) to modify the composition of the soil or eliminate the wetting sources, as in the Valle dei Templi in Agrigento. In this area, the collapsible sand stratum underlying a calcarenitic layer might play a role in the failure mechanisms of the cliffs (Nocilla et al., 2013; Ercoli et al., 2015; Nocilla et al., 2015). Indeed, discontinuities cause an increase in the secondary permeability in the calcarenitic bench (Ercoli et al., 2014) and allow rainwater to flow directly into the underlying sands. For these collapsible sands, it is not possible to use an aqueous stabiliser vehicle (Zimbardo et al., 2016, 2019).

The main purpose of the present study was to stabilise the sand by creating interparticle bonding without triggering structural collapse and causing instability in the overlying structures.

This study was part of a broader research project divided into two phases. In the first, the bonding forces between the textural components of the collapsible sand were investigated, and an appropriate consolidant that did not trigger collapse processes in the metastable structure, was identified (Zimbardo et al., 2016, 2019). The second step, which is presented in this paper, consisted of a laboratory investigation on the effectiveness of non-aqueous mixtures capable of stabilising the structure of the sand, to reduce its collapse potential and improve its strength properties.

Passive stabilising agents were selected to improve the sand's properties by means of the partial occlusion of the inter-assemblage and intergranular spaces. In particular, mixtures of polyethylene glycol and nanolime were selected.

2. Materials: sand and consolidants

Intact sand block samples were taken from the sandy level underlying the calcarenitic bench on which the temples stand (Fig.1a and b). Because of their consistency, a saw was used to separate samples from the cliff face (Fig.1b and c). Then, the blocks were wrapped in plastic wrap and transported to the laboratory in a wooden box. The composition of the sand has been studied in previous investigations by means of thin sections observed by optical microscopy and scanning electron microscopy (SEM) analyses. Based on these previous results for the investigated sand, the bonding mechanism seems to mainly be attributed to capillarity or matric suction forces (Zimbardo et al., 2016). The sand mostly consists of mollusca shell fragments, microfossil esoskeletons, and monocrystalline grains of calcite and quartz. Moreover, assemblages of silt and clay minerals are interposed among them, but microcrystalline carbonate cement is rarely present even at the contact point between grains. In a previous study (Zimbardo et al., 2016), the clay percentage was less than 10 %, with a variability of ± 0.1 % for the tested specimens. The porosity is primarily due to interparticle voids, and subordinately to intraparticle voids, because the microfossil esoskeletons are not usually filled.

Parallelepiped and cylindrical samples were obtained from the blocks for soaking, shear tests, and oedometer tests. Samples were roughly shaped with a knife and then gently smoothed by means of fine grinding paper to reach the final dimensions.

The stabilising agents were selected based on the experiments carried out in the first phase of the research (Zimbardo et al., 2019), which highlighted the ability of PEG to provide the sand with protection, limiting the reduction in volume upon wetting. The eco-compatible polymer PEG600 used in this work is a liquid with a viscosity of 150–190 mPa s at 20 °C, and was provided by Sigma Aldrich.

In order to improve the durability and efficacy of sand stabilisation, the effects of a nanolime mixture were studied. The advantages of using nanolime include reductions in the porosity and water absorption by capillarity (Taglieri et al., 2017).

Nanolimes are dispersions of nanometric particles of calcium hydroxide ($Ca(OH)_2$), mainly in ethanol and isopropanol because these solvents give a more stable dispersion (Borsoi et al., 2016). Based on preliminary solubility tests, only an isopropanol dispersion was used in the present work. CaLoSiL suspensions of isopropanol are currently recommended by the manufacturer for deeper penetration away from the surface (IBZ-Salzchemie Gmbh & Co.KG 2013). The products 'CaLoSiL IP25' (25 g/L of $Ca(OH)_2$) and 'Calosil IP5' (5 g/L of $Ca(OH)_2$) from IBZ-Salzchemie Gmbh & Co.KG were used in the present study, and their characteristics are described in the technical sheet (https://ibz-freiberg.de/downloads/pdf/produkte/sd/eng/msds_CaLoSil_IP.pdf).

In stabilising procedures, one of the main problems is back migration to the surface of the nanolime, due to the alcohol evaporation being faster than the precipitation of the calcium hydroxide (Borsoi et al., 2016). To avoid this process, Niedoba et al. (2017) suggested applying water immediately after the application of nanolime. However, this is, obviously, not possible for collapsible sand. According to the results of previous studies (Zimbardo et al., 2019, 2020), the reduction of the nanolime migration back to the surface is assured by PEG, which ensures an appropriate homogeneous distribution of the nanolime inside the specimen. The stabilising components (PEG and nanolime) were mixed in varying proportions by weight (Table 1). The unit weights of the solid particles of the mixtures ($\gamma_{s,m}$) were calculated according to the following formula:

$$\gamma_{s,m} = \frac{\gamma_{s,P} {}^{*} \gamma_{s,nl}}{\gamma_{s,P} {}^{*} f_{nl} + \gamma_{s,nl} {}^{*} f_P}$$

3. Experimental work

3.1. Impregnation technique

The first step of the stabilisation procedure consisted of preliminary soaking tests to determine the PEG/nanolime ratio to be used for the stabilisation. The penetration depth depended on the application method, and although both methods (brushing and immersion) improved the mechanical properties of the material, the immersion method reached the specimen's core (Graziani et al., 2017).

Table 1
Characteristics of PEG/nanolime mixtures.

Consolidant mixture	Symbol	γ_{sm} [kN/m^3]
PEG600 + 10% IP5	P90_IP5	10.85
PEG600 + 15% IP5	P85_IP5	10.64
PEG600 + 20% IP5	P80_IP5	10.44
PEG600 + 10% IP25	P90_IP25	10.88
PEG600 + 15% IP25	P85_IP25	10.68
PEG600 + 20% IP25	P80_IP25	10.50

The mixture absorption was measured using prismatic sand specimens (20 mm x 25 mm x 18 mm) cut from the same sample and subjected to 3 months of total immersion in a ceramic vessel with the consolidant mixture by monitoring the weight variation. The specimens were gently turned over using tweezers and then weighed (tamponing the excess liquid from the surface) at intervals of time until a constant weight was achieved. According to the preliminary results, all of the samples were impregnated by total immersion.

3.2. Optical and SEM observations

A paired micro-characterisation was used to study the structure and morphology of the soil-additive matrix using optical microscopy and SEM, in order to investigate the effects of adding nanolime on the evolution of soil pore structures and on the variation in the sand microstructure. The instrument used for the SEM observations was an FEI QUANTA 200 FEG, Field Emission Generator, ESEM. Low vacuum, 0.5 mbar water vapour pressure, SEM observations were performed on treated irregular fragments cured at room temperature and relative humidity until the end of the carbonation process in order to better understand the protective mechanism of the treatments.

3.3. Water vapour permeability

The water vapour permeability test evaluated the rate that water vapour flowed through the sand samples. According to the standard procedure (ASTM E96/E96M-16, 2016), a standardised cup was filled with distilled water, leaving a small air gap between the sample (diameter = 33.6 mm, height = 17 mm) and the water. The initial weight of the so-described cup (i.e. consisting of the cup, sample, and water) was measured, and the system was stored in a sealed box filled with silica gel to ensure a value of relative humidity equal to 21 %, which was the value measured inside the testing chamber. Cups were then extracted from the sealed box at regular time intervals and weighed.

3.4. Oedometer tests

Oedometer tests were performed on sand specimens in a saturated state using the conventional consolidation apparatus and standard consolidation tests (ASTM D2435-02, 2002). Specimens with the natural water content were cut from large air-dried blocks of sand and roughly shaped with a knife. To reach a perfect cylindrical shape (38 mm in diameter and 22 mm in height), they were gently smoothed by means of fine grinding paper. The samples were submerged in the consolidant mixture until they reached a constant weight and then dried 20 days under an atmospheric standard condition (carbonation process). Tests were carried out using a conventional 38 mm diameter fixed metal ring oedometer (up to vertical stresses of 14 MPa). Oedometer collapse tests were performed using the same oedometer cell and following the procedure stated by Jennings and Knight (1975).

In these tests, the sample was progressively loaded up to a normal stress (σ_v) equal to 200 kPa and, after 1 h, the cell was flooded with water. The additional change in thickness (ΔH) was then recorded.

3.5. Direct shear tests

Direct shear tests were conducted according to ASTM D3080-98 (1998) (Head, 1998) under a drained condition (Table 5). A 60 mm × 60 mm × 20 mm square specimen was used. Three normal stresses (50 kPa, 100 kPa, and 200 kPa) were applied to determine the shear properties of the untreated and treated sand. The shear loading was applied at a rate of 0.048 mm/min.

Table 2
Results of soaking tests on sand samples impregnated with several PEG600 (P)/ Calosil (IP) solutions.

Mixture	n_m (t = 1 day)	n_m (t = 42 days)	n_m (t = 80days)	γ_m / γ_0
P90_IP5	63	74	70	1.21
P85_IP5	66	82	76	1.21
P80_IP5	71	87	83	1.21
P90_IP25	62	73	75	1.29
P85_IP25	63	75	75	1.27
P80_IP25	45	61	64	1.18
P100	74	74	74	1.23

4. Results

4.1. Impregnation treatment efficacy

In order to evaluate the effectiveness of the impregnation treatments with the different mixtures (Table 2), the ratio (n_m) of the volume of the absorbed mixture and initial porosity of the sample was determined. The volume of the absorbed mixture was calculated by dividing the measured weight increase by the total volume and the specific weight of the mixture. The diagram of Fig. 2, showing the increase in n_m with time, describes the mixture absorption process. It can be observed that n_m grows rapidly during the first hour of soaking (n_m > 60 %). For sand samples soaked in the mixtures with IP25, n_m increases up to a value that is more or less constant after approximately 20–30 days. The mixtures with IP5 seem to have a significant ability to penetrate the sand, with the values of n_m equal to 80 % after 40 days, and then tending to decrease. When the absorption degree is very high, an evaporation phenomenon prevails over the inlet mixture, producing a weight loss of approximately 0.05 g, which could be considered insignificant. The submerged samples did not undergo any collapse. Indeed, no grain detachment during the soaking phase occurred.

In this phase of the research, the criterion for evaluating the suitability of the method was reaching a constant sample weight, indicative of the achievement of a constant degree of absorption, together with the absence of collapse.

The optical and SEM images (Figs. 3 and 4) were taken after 20 days under atmospheric standard conditions, at the end of the nanolime carbonation process.

Optical microscopy made it possible to observe that the stabilising agent uniformly penetrated the sand, creating a cement-film on the grains, and penetrated the small intergranular pores, resulting in the typical ‘contact’ cementation texture between grains and between particle assemblages. Even on the surfaces covered by the cementing film, the larger inter-assemblage voids were not totally occluded (Fig.3). The stabilising treatments connected the sand particles together, partially or totally filling the intergranular voids (Fig. 4a).

The SEM micrographs (Fig. 4a) showed the evident distribution of

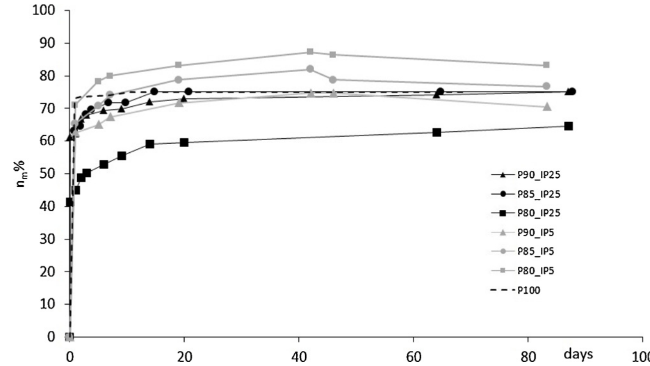

Fig. 2. Impregnation of samples with consolidant mixture: degree of mixture absorption *vs.* time.

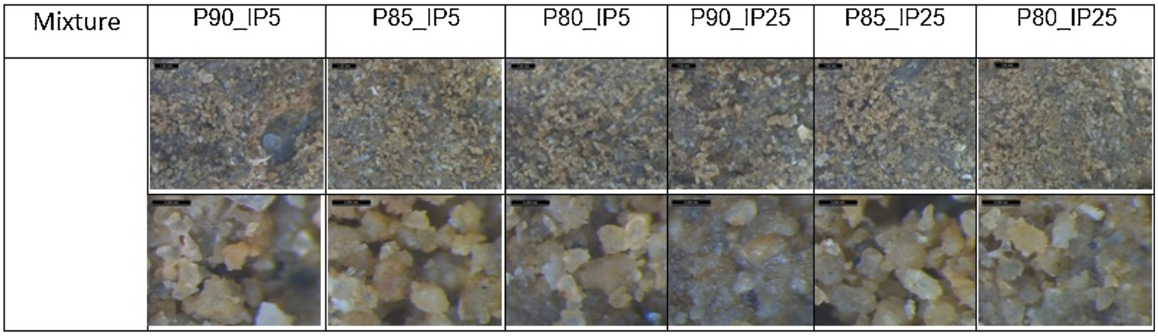

Fig. 3. Optical micrographs of treated sand (first row: lower magnification, second row: higher magnification).

the mixtures inside the specimens. The porosities of the polymer/ nanolime–sand mixtures, both for IP5 and IP25, were lower than that of the natural sand. In particular, the P85_IP5 mixture showed greater efficacy than the P85_IP25 mixture, and smaller pores were filled, resulting in a more continuous structure.

In the untreated sand (Fig. 4b) the calcite crystals that grew on the clasts showed mainly a euhedral shape, whereas in the treated samples, both calcite crystals and clasts appeared to be coated by the mixture. The formed structure increased the bonding by creating bridges between the grain assemblages (Fig. 4c), although the inter-assemblage macroporosity was still open.

According to the results of the previously mentioned soaking tests, as shown in Fig. 2, the treatment with P80_IP25 seemed to be less effective.

a)

Water vapour permeability tests were performed to evaluate the effect of the treatments with the different mixtures on the permeability of the sand. During each test, the weight loss (DW) was calculated with respect to the initial weight and plotted versus time (Fig. 5a). Under steady state conditions, the permeation through the specimens occurred at constant rates. A linear least squares regression was performed to find its slope. In this way, it was possible to determine the rate of vapour flow (DW/Dt) through the specimen, which directly depended on water vapour permeability of the sample. The weight variation rates for different nanolime percentages were determined. The water vapour permeability value of the sand was strongly reduced by the impregnation with PEG, both pure and mixed with nanolime dispersions, as highlighted by the rate vapour flow reduction (Fig. 5b). This result clearly indicated that the PEG tended to reduce the permeability of the sand, while the presence of the nanolime dispersion did not modify this situation; nanolime particles were dispersed in the PEG but did not change the distribution of the polymer within the sand.

4.2. Mechanical improvement

4.2.1. Collapse potential

Experimental investigations of the soil response to wetting are necessary to estimate the collapse settlement at a particular site. Collapse tests were performed to measure the Collapse Potential (CP), as the ratio between the change in specimen height resulting from wetting and the initial specimen height. The results of these collapse tests on the untreated and treated sand are reported in Fig. 6, in which the axial strain (ε_a%) has been plotted versus time. Severe strain changes occurred during the soaking phase of an untreated sample when σ_v was equal to 200 kPa. Indeed, an untreated sample exhibited an immediate collapse onset after soaking in water (Collapse Potential CP = 1.8 %, which corresponded to a moderate risk), whereas for the samples treated with the different mixtures of PEG and nanolime, when flooding with water, the CP value was equal to zero. After 24 h of soaking in water, the CP value was equal to 2.5 % for untreated sand and equal to or lower than 0.6 for the treated sand. For all the treated samples, the axial deformation was lower than that of the untreated sand (Table 3).

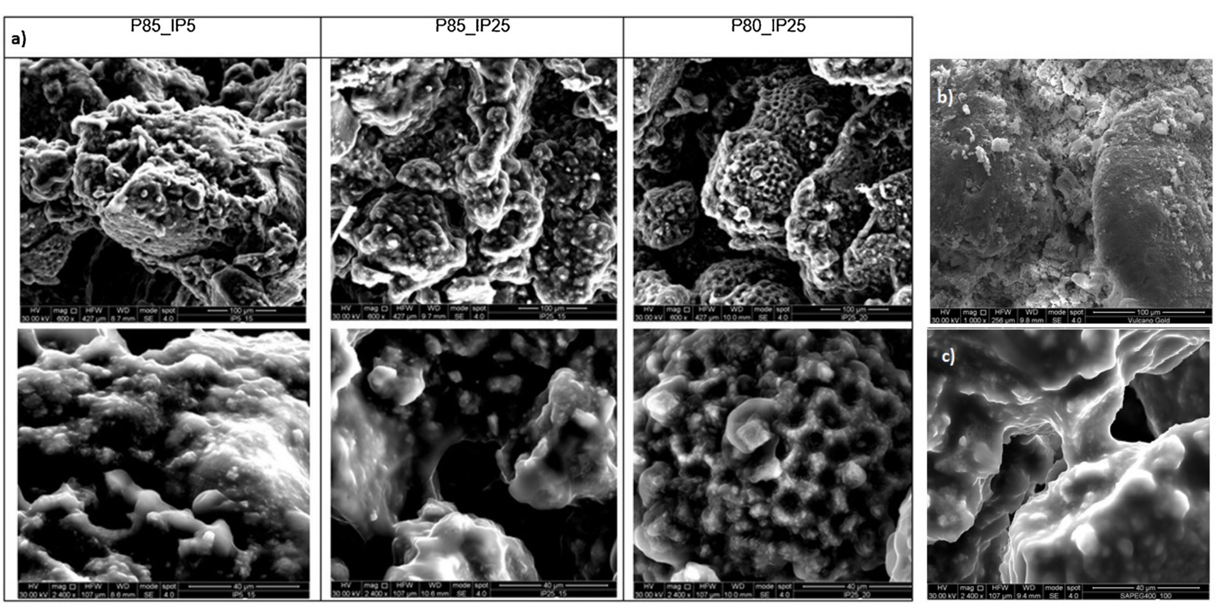

Fig. 4. SEM observations: a)Impregnation of samples with consolidant mixture: (first row: lower magnification of 600x ; second row: higher magnification of 2400x, b) untreated sand magnification of 1000x, and c) bridge of mixture arises between grains (magnification 2400x).

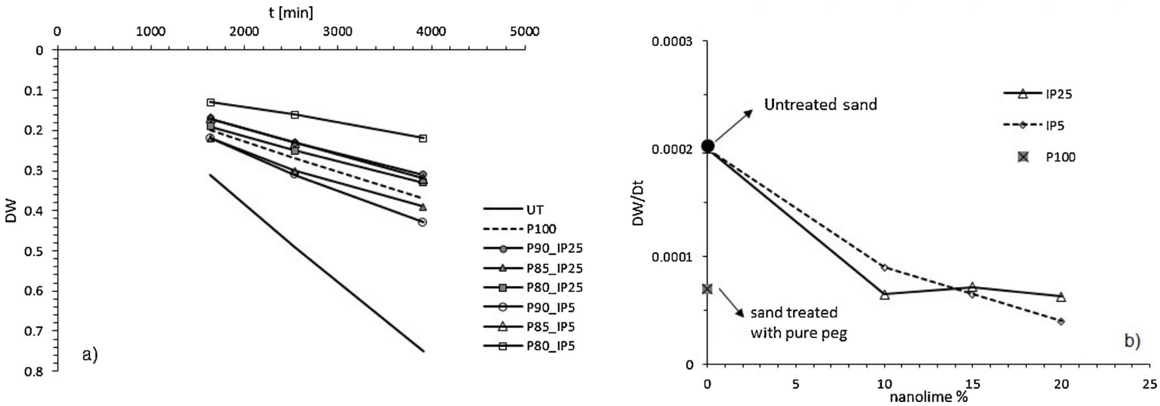

Fig. 5. Water vapour permeability test: a) weight loss (DW) versus time and b) rate of vapour flow versus nanolime percentage.

4.2.2. Compressibility

High-pressure one-dimensional compression tests were performed under wet conditions on natural and treated specimens (Fig. 7). The details of the 12 oedometer tests are given in Table 4. The relationship between the specific volume and the logarithm of the vertical stress for the collapsible sand, both untreated and treated with various amounts of nanolime, are presented in Fig. 7. For the untreated sand, as shown in Fig. 7a, the sample strains do not significantly change up to 200 kPa. At a vertical stress of 200 kPa, the samples were soaked in water and showed changes in strain, as a result of the collapse. The oedometer tests performed on the natural sand showed that the CP increased with the initial specific volume. Just as with bonded soils, the natural sand, under dry condition, had a stress state outside the space permitted for the unstructured soil (Leroueil and Vaughan, 1990). When soil undergoes destructuring, the additional voids ratio sustained by suction decreases. After wetting, the sand's behaviour was like that of loose soil and, at high stress levels, it was possible to identify a unique one-dimensional Normal Compression Line (1D-NCL) in the v-log σ'_v plane (Fig. 7a).

When soaked in water, the samples treated with PEG exhibited CP values equal to zero (Fig. 7b). Thus, PEG impregnation appeared to offer a considerable protection against water, strengthening the contacts between soil particles. After soaking, for a given vertical stress, the void ratio for the PEG treated samples was higher than that of the natural soil with a similar initial specific volume.

The treatment with pure PEG reduced the compressibility of the sand, and the effect became less important as the deformation process developed. For stresses higher than 8 MPa, regardless of the initial void ratio, the compression curves tended to converge to the 1D-NCL. The addition of a small amount of nanolime to the collapsible sand not only reduced the collapse-induced volume changes, as seen in Fig. 6, but also increased the range of elastic behaviour. It can be observed in Fig. 7c that as the nanolime (IP25) percentage decreases, the initial specific volume of the treated sample decreases. In contrast, for samples treated with nanolime IP5 (Fig. 7d) the lowest initial specific volume is achieved for the sample treated with 20 % nanolime.

Table 3
Results of oedometer collapse tests at σ_v equal to 200 kPa on sand samples impregnated with several PEG600 (P)/Calosil (IP) solutions.

Test	Liquid at 200KPa	CP [%] at 0.25 min after soaking	CP [%] at 1440 min after soaking	ε_a % t = 10,000 min
CT1D- untreated sample	water	1.8	2.5	3.40
CT1D-P1002	water	0	0.45	0.90
CT1D-P90_IP25	water	0	0.5	0.80
CT1D-P85_IP25	water	0	0.4	0.81
CT1D-P80_IP25	water	0	0.6	1
CT1D-P90_IP5	water	0	0.2	0.62
CT1D-P85_IP5	water	0	0.3	0.52
CT1D-P80_IP5	water	0	0.5	0.74

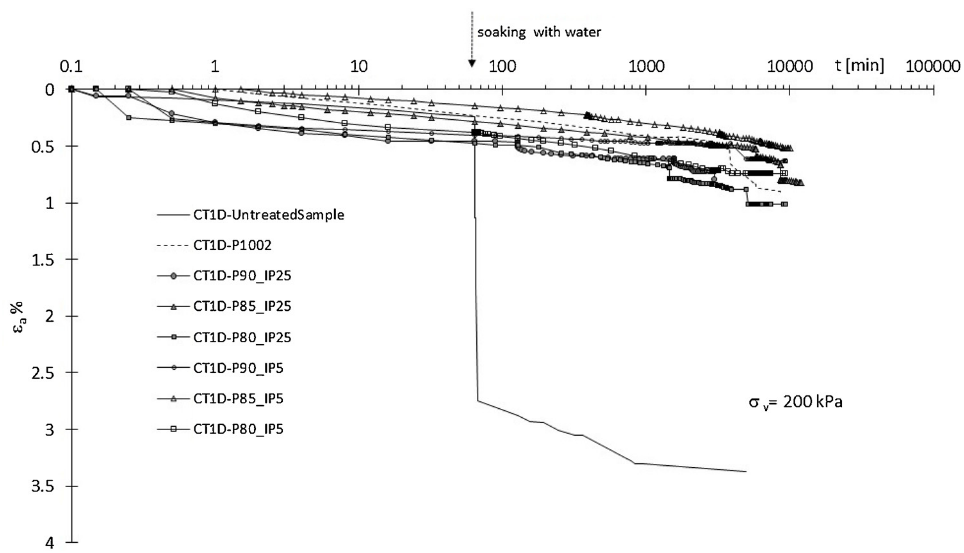

Fig. 6. Oedometer collapse tests (CT) with σ_v = 200 kPa.

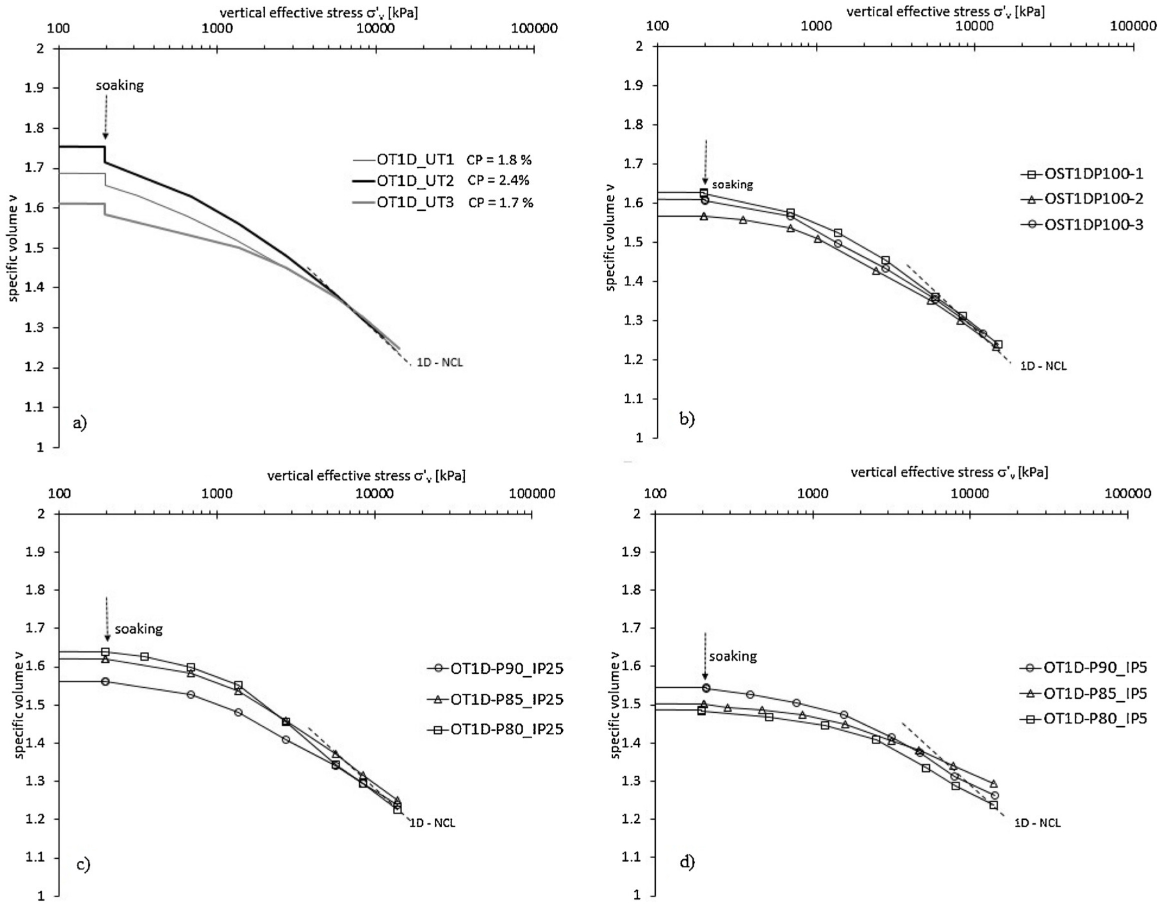

Fig. 7. Results of oedometer tests on a) natural samples, b) sand treated with pure PEG, c) sand treated with different mixtures of PEG and Calosil IP25, and d) sand treated with different mixtures of PEG and Calosil IP5.

Table 4
Results of oedometer tests on untreated sand samples and those impregnated with different mixtures soaking in water at σ_v equal to 200 kPa.

Test	v_0	σ'v [MPa]	Cc	Cr
OT1D_UT1	1.69	14	0.35	0.18
OT1D_UT2	1.76	14	0.35	0.19
OT1D_UT3	1.62	14	0.33	0.14
OT1D-P100_1	1.64	14	0.30	0.09
OT1D-P100_2	1.63	14	0.27	0.08
OT1D-P100_3	1.62	14	0.28	0.085
OT1D-P90_IP25	1.56	14	0.24	0.05
OT1D-P85_IP25	1.62	14	0.29	0.08
OT1D-P80_IP25	1.64	14	0.30	0.07
OT1D-P90_IP5	1.55	14	0.21	0.06
OT1D-P85_IP5	1.50	14	0.17	0.05
OT1D-P80_IP5	1.49	14	0.20	0.04

Table 5
Direct shear test results for untreated and treated (P85_IP5) sand.

Test	Shear strength [kPa]			Shear strength parameters	
	σ'v = 50 kPa	σ'v = 100 kPa	σ'v = 200 kPa	c' [kPa]	Φ'
SH_UT1	75	117	204	33	40°
SH-P85_IP5	156	210	293	114	42°

For all dosages of nanolime, the change in the void ratio was very small in the stress range before the respective yield stress. At the post-yield stress phase, the reduction of the void ratio was likely due to the breaking of bonds. In general, the treatment with IP5 seemed to have a greater effect on the structural changes. Indeed, the compression curves corresponding to the samples treated with PEG and CalosilIP5, in any proportions, at high stresses, came above the normal compression line of the natural sand, thus indicating a behaviour similar to that of structured soils. These samples showed a non-convergent compression behaviour, which indicated structural changes due to the treatment.

In order to compare the compressibility behaviours at different nanolime percentages, the consolidation data were analysed in terms of the axial strain (ε_a)(Fig. 8a). It was evident that the presence of the consolidant was beneficial to improve the interparticle bonds between grains. The treatments rendered the soil less compressible. Indeed, the ultimate strain (at 14 MPa compression) ranged between 14 % for a sample treated with 15 % nanolime IP5 and 25 % for a sample treated with 20 % nanolime IP25. Therefore, compared with the natural untreated sand, the deformation was reduced by 45 %. Fig. 8 shows the role played by the nanolime dosage and the effect of the mixture-treated sand on the compressibility parameters. The variations of the compression index (Cc) and re-compression index (Cr) of the sand/mixture system as functions of the nanolime concentration are also shown in Fig. 8b and c. It can be seen that Cc and Cr decrease with an increase in the nanolime content.

4.2.3. Shear strength

Laboratory shear tests were conducted on the sand treated with the P85_IP5 mixture, which exhibited a lower compressibility in the oedometer tests.

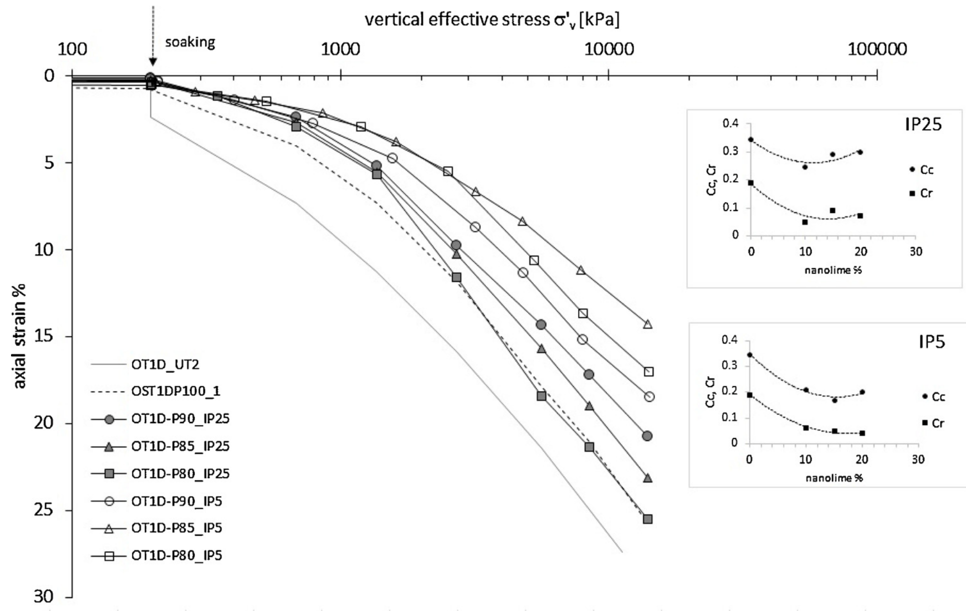

Fig. 8. Oedometer tests results: a) axial strain versus vertical stress, b) Cc and Cr variations for different nanolime IP25 percentages, and c) Cc and Cr variations for different nanolime IP5 percentages.

The effects of the stabilisation on the shear stress–strain behaviours of the treated and untreated sand associated with the Mohr-Coulomb failure envelopes are presented in Fig. 9. It is readily observed that the mixture improves the overall behaviour of the treated soil, because it increases the peak strength at each normal stress. As expected, the shear stress increases monotonically with an increase in the shear displacement before the peak shear strength is reached. After the peak, the shear stress trends are similar for the direct shear tests carried out on treated and untreated soil. Compared to the untreated sand at the same effective vertical stress, the failure shear stress of the treated samples is achieved for greater shear displacement values, demonstrating the greater adhesion between grains. Fig. 9a shows that with an increase in the effective normal stress, both the improvement in the shear strength and the increase in the horizontal displacement at the peak (horizontal displacement at peak of treated sand/horizontal displacement at peak of untreated sand) decrease.

This behaviour can be attributed to the redistribution of the mixture–sand fabric. Indeed, the addition of PEG and nanolime strengthening the bond between the soil particles causes changes in the soil texture.

The failure envelopes corresponding to the shear strengths obtained from the direct shear tests are presented in Fig. 9b. The observed shear parameters (cohesion c' and angle of shearing resistance φ') indicate that the treated soil exhibits an increase in the cohesion (c'). The treatment seems to have little effect on the angle of shearing resistance φ'; the two envelopes are parallel. In contrast, the stabiliser mixture gives a greater cohesion intercept c´ to the strength envelope (Table 5).

4.2.4. Discussion

To examine the effects of the stabiliser mixtures on the soil structure evolution of the intact sand, the treated sand was analysed using optical and SEM observations (Figs. 3 and 4). The images of the samples, stabilised with the mixture, revealed that in addition to the partial filling of the interparticle voids, a film that covered the clasts was formed.

Moreover, the grains were now bonded with new calcium carbonate particles that originated with the carbonation process of the introduced nanolime. Such calcite microcrystals formed little bridges of cementation between the original grains (Fig. 4c). The influence of the stabiliser mixtures is noticeable on the compression curve (Fig. 7), where the stress–strain relationships are compared with that of the untreated sand.

The obtained results highlighted the efficacy of the treatment in reducing the structural collapse of the sand upon wetting. This reduction could be attributed to the presence of PEG, which enveloped the sand grains and acted as a barrier with respect to the water inlet, as already observed by Zimbardo et al. (2019). The effect of the nanolime

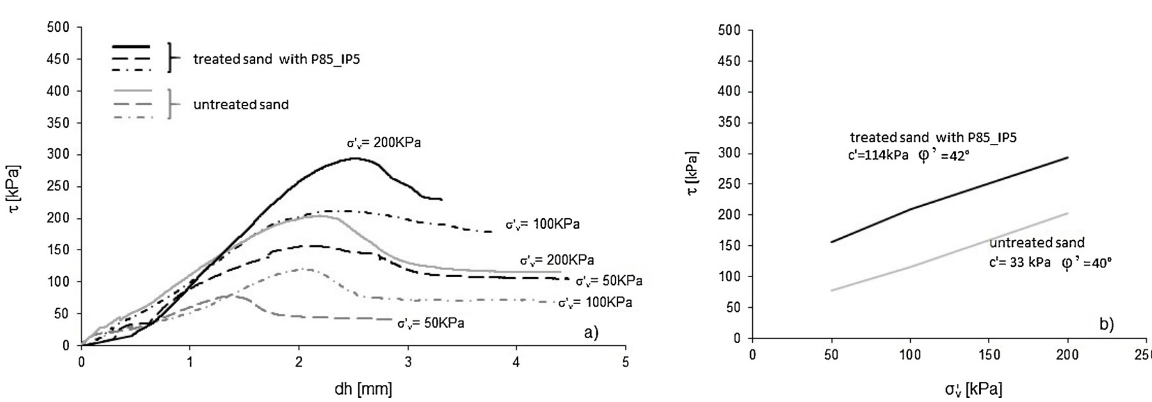

Fig. 9. Effect of mixture stabilisation on shear stress–strain behaviour of sand: a) shear stress versus horizontal displacement for natural sand and sand treated with P85_IP5 mixture and b) peak failure envelopes for natural sand and sand treated with P85_IP5 mixture.

on the compressibility was evident. In the case of the treatment with the P85_IP5 mixture, which was the best stabilising treatment among those tested, the curve in the v- σ_v' plane had a higher post-yield specific volume (Fig. 7d).

Particle breakage has often been associated with time effects and stress levels in granular materials (Lade et al., 2010). Grain crushing is negligible at very low stresses but becomes significant with increasing pressure and time effects. In this work, particle crushing in the Agrigento sand samples was investigated by means of an optical microscopy analysis, and no breakage seemed to occur, with no fresh broken surface detectable. The grains remained intact both in the untreated and treated sand, despite the high level of stress reached during the tests. Because the clasts were not affected by fracturing, the mineralogic composition of the studied sand did not seem to influence the deformation process during the oedometer tests. Therefore, the deformations were attributable to changes in the structural features. Producing higher stress levels to induce grain breakage was beyond the aims of this study. However, future investigations on the time effect and relative breakage, within a wide range of stresses, should be planned for this purpose.

In the present work, the author's purpose was to evaluate the effects of treatments with stabilising mixtures on the collapse potential and compressibility of the sand. In order to make this comparison, the same procedure used to calculate the CP was adopted. It was clear that the treatment could affect the matric suction. However, under identical boundary conditions, only the macroscopic effect of the treatment on the compressibility was analysed in this study, rather than the different mechanical responses to the matric suction variations.

5. Conclusion

This paper presented the stabilising effects of different consolidant mixtures on the mechanical behaviour of collapsible sand. From the data presented in this paper, the stabilised sand had a higher shear strength, lower water vapour permeability, and lower compressibility than natural soil, and the following conclusions could be drawn:

- when the natural sand became wet, the soil's strength was compromised, causing collapse; the stabilising mixtures developed bonding, increasing the interlocking forces between sand particles within the soil structure, and thus allowed it to resist collapse when wetted.
- The stabiliser treatment decreased the water vapour permeability and void ratio of the sand, without significantly occluding the pores.
- PEG ensured an appropriate homogeneous distribution of the nanolime inside the specimen reducing the back migration of nanolime; adding a small amount of nanolime to collapsible sand not only reduced the collapse-induced volume changes, but could also increase the 'elastic' behaviour of the soil and effectively improve the shear strength parameters of the collapsible sand. There was a considerable increase in cohesion, with little effect on the angle of shearing resistance.
- The mixtures with PEG and nanolime IP5 seemed to have a greater influence on the structure of the sand, and the tests showed that the behaviour of the treated samples was similar to that of structured soil. At a high stress, the treated IP5 sand had an higher void ratio (i.e. the compression curve came above the normal compression line of the natural sand). This additional void ratio showed the influence of the soil structure (Burland, 1990). Further, the compression curves showed a non-convergent compression behaviour, indicating the structural changes due to the treatment.

It can be concluded that the treatment with PEG and nanolime prevented collapse and acted like a bonding agent. Thus, the stabilised sand exhibited a new fabric arrangement different from that of natural sand. According to the results, the treatment improved the mechanical behaviour of the sand, and the P85_IP5 mixture appeared to provide the best stabilising treatment among those tested. The acquired results showed that the PEG and nanolime treatment could improve the mechanical behaviour of the soil with respect to water action, resulting in the prolonged stability of the soil foundation.

This preliminary achievement requires further study to assess the influence that several factors could have on the long-term efficacy, including the pore network, nanolime concentration, nature of the solvent, time, and application method. Field tests are necessary to identify the best method for applying the stabiliser mixture in the field.

Declaration of Competing Interest

None.

Acknowledgments

This work was financially supported by the PRIN program within the project 'Monitoraggio, consolidamento, conservazione e protezione dei beni culturali n. 2015WBEP3H' and carried out within a cooperation protocol between the DICAM department and the 'Parco Archeologico e Paesaggistico della Valle dei Templi' authority.

References

Al-Khanbashi, A., El-Gamal, M., 2003. Modification of sandy soil using waterborne polymer. J. Appl. Polym. Sci. 88, 2484–2491.

Al-Rawas, A.A., 2000. State of the art review of collapsible soils. Sci. Technol. Special Rev. 115–135.

Anayev, V.P., Volyanick, N.V., 1986. Engineering geologic peculiarities of construction work on loessial soils. Proc., 5th Int. Cong. of Association of Engineering Geologists, 2, Buenos Aires.

ASTM D3080-98, 1998. Standard test method for direct shear test of soils under consolidated drained conditions. Annual Book of ASTM Standards, vol. 04.08. ASTM International, West Conshohocken, PA 1–6.

ASTM E96/E96M-16, 2016. Standard Test Methods for Water Vapor Transmission of Materials. ASTM International, West Conshohocken, PA.

Aurisicchio, S., Evangelista, A., Nicolais, L., 1985. Comportamento Meccanico Del Tufo Trattato Con Polimeri. Rivista Italiana di Geotecnica, pp. 89–100.

Barden, L., Mcgown, A., Collins, K., 1973. The collapse mechanism in partly saturated soil. Geotech. Eng. 7 (1), 49–60.

Borsoi, G., Lubelli, B., van Hees, R., Rosário Veigac, R., Silva, A.S., 2016. Understanding the transport of nanolime consolidants within Maastricht limestone. J. Cult. Herit. 18, 242–249.

Burland, J.B., 1990. On the compressibility and the shear strength of natural clays. Gotechnique 40, 329–378.

Cintra, J.C.A., Nogueira, J.B., Filho, F.C., 1986. Shallow foundations on collapsible soils. In: Proc., 5th Int. Cong., Int. Association of Eng. Geologists, Buenos Aires. pp. 673–675.

Clemence, S.P., Finbarr, A.O., 1981. Design considerations for collapsible soils. J. Geotech. Eng. Div. https://doi.org/10.1016/0148-9062(81)91226-2.

Daniele, V., Taglieri, G., Quaresima, R., 2008. The nanolimes in cultural heritage conservation: characterisation and analysis of the carbonatation process. J. Cult. Herit. 9, 294–301.

Dei, L., Salvadori, B., 2006. Nanotechnology in cultural heritage conservation: nanometric slaked lime saves architectonic and artistic surfaces from decay. J. Cult. Herit. 7, 110–115.

Drdácký, M., Slížková, Z., Ziegenbalg, G., 2009. A nano approach to consolidation of degraded historic lime mortars. J. Nano Res. 8, 13–22.

Dudley, J.H., 1970. Review of collapsing soils. J. Soi. Mech. Found.,Div. ASCE 96 (3), 925–947.

Ercoli, L., Zimbardo, M., Nocilla, N., Nocilla, A., Ponzoni, E., 2015. Evaluation of cliff recession in the Valle dei Templi in Agrigento (Sicily). Eng. Geol. 192, 129–138.

Ercoli, L., Zimbardo, M., Nocilla, A., 2014. Rock decay phenomena and collapse processes in the "Latomiae del Paradiso" in Syracuse (Sicily). Eng. Geol. 178, 155–165.

Feda, J., 1966. Structural stability of subsident loess soil from Praha-Dejvice. Eng. Geol. 1, 201–219.

Gallagher, P.M., Lin, Y., 2005. Column testing to determine colloidal silica transport mechanisms. In: Texas. Proc. Sessions of the Geo-Frontiers Congress of Innovations in Grouting and Soil Improvement 162. pp. 1–10.

Gao, G., 1996. The distribution and geotechnical properties of loess soils, lateritic soils and clayey soils in China. Eng. Geol. 42 (1), 95–104.

Garakani, A.A., Haeri, S.M., Khosravi, A., Habibagahi, G., 2015. Hydromechanical behavior of undisturbed collapsible loessial soils under different stress state conditions. Eng. Geol. 195, 28–41.

Giorgi, R., Ambrosi, M., Toccafondi, N., Baglioni, P., 2010. Nanoparticles for cultural heritage conservation: calcium and barium hydroxide nanoparticles for wall painting consolidation. Chem. Eur. J. 16 (31), 9374–9382.

Graziani, G., Sassoni, E.W., Scherer, G., Franzoni, E., 2017. Penetration depth and redistribution of an aqueous ammonium phosphate solution used for porous limestone consolidation by brushing and immersion. Constr. Build. Mater. 148, 571–578.
Haeri, S.M., Zamani, A., Garakani, A.A., 2012. Collapse potential and permeability of undisturbed and remolded loessial soil samples. Unsaturated soils: Research and applications, 301-308. Springer, Berlin, Heidelberg.
Haeri, S.M., Garakani, A.A., 2012. The variation of total volume change, water volume change, yielding net confining stress and shear strength of undisturbed unsaturated loess under isotropic compression. Unsaturated Soils: Research and Applications. Springer, Berlin, Heidelberg, pp. 293–300.
Haeri, S.M., Hosseini, A.M., Shahrabi, M.M., Soleymani, S., 2015. Evaluation and comparison of strength characteristics of Gorgan loessial soil improved with nano-silica, lime and Portland cement. 15th Pan-American Conference on Soil Mechanics and Geotechnical Engineering, Buenos Aires, Argentina. https://doi.org/10.3233/978-1-61499-603-3-1820.
Haeri, S.M., Khosravi, A., Garakani, A.A., Ghazizadeh, S., 2016. Effect of soil structure and disturbance on hydromechanical behavior of collapsible loessial soils. Int. J. Geomech. 17 (1).
Haeri, S.M., Garakani, A.A., Roohparvar, H.R., Desai, C.S., Seyed Ghafouri, S.M.H., Salemi Kouchesfahani, K., 2019. Testing and constitutive modeling of limestabilized collapsible loess. I: experimental investigations. Int. J. Geomech. 19 (4), 04019006.
Hansen, L.A., Booth, R.D., Beckwith, G.H., 1989. . Characterization of a Site Underlain by Deep Collapsing Soils. Foundation Engineering: Current Principles & Practices, 1. ASCE, New York, pp. 191–208.
Head, K.H., 1998. Manual of Soil Laboratory Testing, vol. 3, second ed. John Wiley and sons.
Hosseini, S.E., Alizadeh, M.K., Mesbah, A., 2012. Evaluation of shear strength parameters of amended loess through using common admixtures in Gorgan, Iran. . World Acad. Sci. Eng. Tech. Int. J. Struct. Constr. Eng. 6.
Houston, S.L., Houston, W.N., 1997. Collapsible Soils Engineering. Unsaturated Soil Engineering Practice, Geotechnical Special Publication, 68. ASCE.
Houston, S.L., Houston, W.N., Zapata, C.E., Lawrence, C., 2001. Geotechnical engineering practice for collapsible soils. In: Toll, D.G., Augarde, C.E., Gallipoli, D., Wheeler, S.J. (Eds.), Soil Concepts and Their Application in Geotechnical Practice. Springer, Netherlands, pp. 333–355.
Idrees, M., Batool, S., Kong, J., Zhuang, Q., Liu, H., Shao, Q., Lu, N., Feng, Y., Wujcik, E.K., Gao, Q., Ding, T., Wei, R., Guo, Z., 2019. Polyborosilazane derived ceramics - Nitrogen sulfur dual doped graphene nanocomposite anode for enhanced lithium ion batteries. Electrochim. Acta 296, 925–937 ISSN 0013-4686.
Jennings, J.E., Knight, K., 1975. A guide to construction on or with materials exhibiting additional settlement due to collapse of grain structure. Proc., 6th African Conf. on Soil Mechanics and Foundation Engineering 99–105.
Jiang, D., Murugadoss, V., Wang, Y., Lin, J., Ding, T., Wang, Z., Shao, Q., Wang, C., Liu, H., Lu, N., Wei, R., Subramania, A., Guo, Z., 2019. Electromagnetic interference shielding polymers and nanocomposites - a review. Polym. Rev. 59 (2), 280–337. https://doi.org/10.1080/15583724.2018.1546737.
Kakavand, A., Dabiri, R., 2018. Experimental study of applying colloidal nano Silica in improving sand-silt mixtures. Int. J. Nano Dimens. 9, 357–373.
Kazemi, M., 2010. Using deep soil mixing method for stabilizing the wake of the collapse of the soil. 11th Confer. of Construction and Project Management, Iran 25–34.
Lade, P., Nam, J., Liggio Jr., C., 2010. Effects of particle crushing in stress drop-relaxation experiments on crushed coral sand. J. Geotech. Geoenviron. Eng. 136 (3), 500–509.
Leroueil, S., Vaughan, P.R., 1990. The general and congruent effects of structure in naturalsoils and weak rocks. Gotechnique 40, 467–488.
Lin, Z., Lin, B., Wang, Z., et al., 2019. Facile preparation of 1T/2H-Mo(S1-xSex)2 nanoparticles for boosting hydrogen evolution reaction. Chemcatchem 11, 2217.
Lutenegger, A.J., Hallberg, G.R., 1988. Stability of loess. Eng. Geol. 25, 247–261.
Mitchell, J.K., 1976. Fundamentals of Soil Behavior. Wiley, New York, pp. 437–444.
Niedoba, K., Slížková, Z., Frankeová, D., Lara Nunes, C., Jandejsek, I., 2017. Modifying the consolidation depth of nanolime on Maastricht limestone. Constr. Build. Mater. 133, 51–56.
Nocilla, N., Ercoli, L., Zimbardo, M., Nocilla, A., Meli, P., Grado, G., Parello, G., Presti, G., 2013. Unsaturated sand in the stability of the cuesta of the temple of hera (Agrigento). Proc. 2nd International Symposium on Geotechnical Engineering for the Preservation of Monuments and Historic Sites 603–611.
Nocilla, N., Zimbardo, M., Ercoli, L., Nocilla, A., Ponzoni, E., 2015. Collapsible soils and instability processes in the Valle dei Templi (Agrigento). Rivista Italiana di Geotecnica. 49 (1), 65–78.
Noll, M.R., Bartlett, C., Dochat, T.M., 1992. In situ permeability reduction and chemical fixation using colloidal silica. In: Proc. 6th National Outdoor Action Conference on Aquifer Restoration, Ground Water Monitoring, and Geophysical Method. Las Vegas. pp. 443–457.
Otero, J., Starinieri, V., Charola, A.E., 2018. Nanolime for the consolidation of lime mortars: a comparison of three available products. Constr. Build. Mat. 181, 394–407.
Pengelly, A.D., Boehm, D.W., Rector, E., Welsh, J.P., 1997. engineering experience with in-situ modification of collapsible and expansive soils. Unsaturated soil engineering practice. In: ASCE Geotechnical Special Publication, Proc. First Geo Institute Conference. Logan, UT, USA, July 15-17, Part 68. pp. 277–298.
Pereira, J.H., Fredlund, D.G., Cardão Neto, M.P., Gitirana Jr., G.D.F., 2005. Hydraulic behavior of collapsible compacted gneiss soil. J. Geotech. Geoenviron. Eng. 131, 1264–1273.
Ping, L., Sai, V., Tonglu, L., 2016. Review of collapse triggering mechanism of collapsible soils due to wetting. J. Rock Mech. Env. Eng. 8, 256–274.
Rizzo, G., Ercoli, L., Megna, B., 2009. Effectiveness of preservative treatments on coloured ruditic building stones. Strain 45 (5), 424–432.
Rollins, K.M., Rogers, G.W., 1994. Mitigation measures for small structures on collapsible alluvial soils. J. Geotech. Eng. 120 (9) 1533.
Romero, E., Simms, P.H., 2008. Microstructure investigation in unsaturated soils: a review with special attention to contribution of mercury intrusion porosimetry and environmental scanning electron microscopy. J. Geotech. Geoenviron. Eng. 26, 705–727.
Saad, I.S., Amal, A.S., Taie, A.H.A.L., 2016. Influence of nano additives on unconfined compressive strength of asphaltic soil. Chem. Biom. Eng. 1, 32–39.
Steward, P.A., Hearn, J., Wilkinson, M.C., 2000. An overview of polymer latex film formation and properties. Adv. Colloid Interface Sci. 86, 195–267.
Taglieri, G., Oterob, J., Daniele, V., Gioia, G., Macera, L., Starinieri, V., Charola, A.E., 2018. The biocalcarenite stone of Agrigento (Italy): Preliminary investigations of compatible nanolime treatments. J. Cult. Herit. 30, 92–99.
Taglieri, G., Daniele, V., Rosatelli, G., 2017. Eco-compatible protective treatments on an Italian historic mortar (XIV century). J. Cult. Herit. 25, 135–141.
Yonekura, R., Miwa, M., 1993. Fundamental properties of sodiumsilicate based grout. In: Proc. 11th Southeast Asian Geotech. Conf. Singapore. pp. 439–440.
Zeng, G., Meng, X., 2006. Experimental study on the relationship between moisture content and deformation of collapsible loess. In: Ning, L., Laureano, R. (Eds.), Advances in Unsaturated Soil, Seepage, and Environmental Geotechnics, Geotechnical Specia lPublications. ASCE, pp. 136–142.
Zhang, G., Germaine, J.T., Whittle, A.J., Ladd, C.C., 2004. Index properties of a highly weathered old alluvium. Gotechnique 54, 441–451.
Zhu, G., Cui, X., Zhang, Y., Chena, S., Dong, M., Liu, H., Shao, Q., Ding, T., Wu, S., Guo, Z., 2019. Poly (vinyl butyral)/Graphene oxide/poly (methylhydrosiloxane) nanocomposite coating for improved aluminum alloy anticorrosion. Polymer 172, 415–422.
Ziaie Moayed, R., Kamalzare, M., 2015. Improving physical characteristics of collapsible soil (Case study: tehran-semnan railroad). J. Eng. Geo. 9, 2.
Zimbardo, M., Ercoli, L., Megna, B., 2016. The open metastable structure of a collapsible sand: fabric and bonding. Bull. Eng. Geol. Environ. 75 (1), 125–139.
Zimbardo, M., Ercoli, L., Megna, B., Scaffaro, R., 2019. Collapsibility of metastable sand by non-conventional oedometer tests. Gran. Matt. 21 (1).
Zimbardo, M., Nocilla, A., Coop, M.R., Ercoli, L., Megna, B., Mistretta, M.C., 2020. The effects of structure on the one dimensional compression behaviour of a porous calcarenite. In: Calvetti, F., Cotecchia, F., Galli, A., Jommi, C. (Eds.), Geotechnical Research for Land Protection and Development. CNRIG 2019. Lecture Notes in Civil Engineering, 40. Springer, Cham.